Received: 19 August 2016 | Accepted: 26 January 2017

DOI: 10.1111/fog.12214

ORIGINAL ARTICLE

WILEY FISHERIES OCEANOGRAPHY

# Influence of oceanographic conditions on abundance and distribution of post-larval and juvenile carangid fishes in the northern Gulf of Mexico

John A. Mohan[1] | Tracey T. Sutton[2] | April B. Cook[2] | Kevin M. Boswell[3] | R. J. David Wells[1,4]

[1]Department of Marine Biology, Texas A&M University at Galveston, Galveston, TX, USA

[2]Department of Marine and Environmental Sciences, Nova Southeastern University, Dania Beach, FL, USA

[3]Department of Biological Sciences, Florida International University, North Miami, FL, USA

[4]Department of Wildlife and Fisheries Sciences, Texas A&M University, College Station, TX, USA

**Correspondence**
John A. Mohan
Email: jmohan@tamu.edu

**Funding information**
Gulf of Mexico Research Initiative; National Oceanic and Atmospheric Administration

## Abstract

Relationships between abundance of post-larval and juvenile carangid (jacks) fishes and physical oceanographic conditions were examined in the northern Gulf of Mexico (GoM) in 2011 with high freshwater input from the Mississippi River. Generalized additive models (GAMs) were used to explore complex relationships between carangid abundance and physical oceanographic data of sea surface temperature (SST), sea surface height anomaly (SSHA) and salinity. The five most abundant carangid species collected were: *Selene setapinnis* (34%); *Caranx crysos* (30%); *Caranx hippos* (10%); *Chloroscombrus chrysurus* (9%) and *Trachurus lathami* (8%). Post-larval carangids (median standard length [SL] = 10 mm) were less abundant during the spring and early summer, but more abundant during the late summer and fall, suggesting summer to fall spawning for most species. Juvenile carangid (median SL = 23 mm) abundance also increased between the mid-summer and early fall. Most species showed increased abundance at lower salinities and higher temperatures, suggesting entrainment of post-larval fishes or feeding aggregations of juveniles at frontal convergence zones between the expansive river plume and dynamic mesoscale eddy water masses. However, responses were species- and life-stage specific, which may indicate fine-scale habitat partitioning between species. Ordination methods also revealed higher carangid abundances at lower salinities for both post-larval and juvenile life stages, with species- and life-stage specific responses to SST and SSHA, further suggesting habitat separation between species. Results indicate strong links between physical oceanographic features and carangid distributions in the dynamic northern GoM.

**KEYWORDS**
Carangidae, generalized additive models, Gulf of Mexico, large midwater trawl, Mississippi River, MOC

## 1 | INTRODUCTION

Physical oceanographic features structure marine communities through bottom-up trophic interactions and passive concentration mechanisms (Godø et al., 2012; Lima, Olson, & Doney, 2002; Lindo-Atichati et al., 2012; Meekan et al., 2006; Williams, Mcinnes, Rooker, & Quigg, 2015). Oceanic currents and eddies occur over diverse spatial scales and interact over various temporal scales (Hamilton, 1992; Vukovich, 2007). Hydrodynamic convergence and turbulent mixing supply nutrients in otherwise oligotrophic waters, fueling

  

primary production and transferring energy to higher trophic levels (Bakun, 2006). In the northern hemisphere, anticyclonic warm core eddies spin clockwise causing downwelling and are considered nutrient-depleted (Biggs, 1992). Cyclonic cold core eddies spin counterclockwise, resulting in upwelling that introduces new nitrogen into the base of the mixed layer (Biggs, 1992; Seki et al., 2001). Frontal zones occur at the confluence of anticyclone/cyclone eddy pairs and are often associated with increased primary and secondary production that may be advected to remote offshore locations (Toner et al., 2003).

The Gulf of Mexico (GoM) is a semi-enclosed intercontinental sea with a unique circulation that is controlled by the intrusion of the Loop Current (LC) comprising warm water from the Caribbean Sea that enters through the Yucatan Strait and exits through the Straits of Florida. As the LC extends into the eastern GoM, anticyclonic warm-core mesoscale eddies are shed and transported westward into the central and western GoM (Biggs, 1992; Vukovich & Crissman, 1986). Frictional interactions of warm-core eddies with the steep topography of the continental slope form cyclonic/anticyclonic eddy pairs (Biggs & Müller-Karger, 1994; Hamilton, 1992). The physical characteristics of mesoscale features and fronts including sea surface height anomaly (SSHA), sea surface temperature (SST), salinity and nutrient gradients influence the distribution of primary producers and subsequent secondary consumers including larval and juvenile fishes (Grimes & Finucane, 1991; Rooker et al., 2013). Additionally, discharge from the Mississippi River, which drains two-thirds of the US continent, delivers low salinity, nutrient-rich water into the northern GoM that enhances primary and secondary productivity in nearshore waters (Chesney, Baltz, & Thomas, 2000; Grimes, 2001). Increased nitrate and chlorophyll concentrations resulting from mesoscale circulation, are thought to support enhanced zooplankton and nekton biomass (Zimmerman & Biggs, 1999).

In the northern GoM, the Mississippi River plume is a dominant feature that can extend over 400 km to offshore oceanic regions (Del Castillo et al., 2001). The transport of terrestrial enriched river discharge with high levels of "new" nitrate (Dagg & Breed, 2003) results in high fishery production in the northern GoM (Chesney et al., 2000; Grimes, 2001). In 2011, record flooding of the Mississippi River with a peak discharge of 40,000 $m^3$ $s^{-1}$ in May that was twice the 60 year mean (Walker, Wiseman, Rouse, & Babin, 2005), resulted in an expansive plume that was identifiable with satellite measurements (Falcini et al., 2012; Gierach, Vazquez-Cuervo, Lee, & Tsontos, 2013). Nitrate levels recorded in the far-field plume of the Mississippi River ranged from 5 to 10 μM (Dagg & Breed, 2003; Lohrenz et al., 1999) and are comparable to nitrate concentrations measured in cyclonic eddies in the GoM at 100 m depth ranging from 11 to 15 μM (Biggs & Müller-Karger, 1994; Zimmerman & Biggs, 1999). Thus, cyclonic eddies and the river plume features may support similar levels of primary and secondary production and provide enhanced food for larval and juvenile fishes.

The Carangidae (jack) family of fishes occurs worldwide throughout tropical and temperate waters, primarily occupying the epipelagic (upper 200 m) water column. Most fishes in the family Carangidae form large schools that prey upon shrimps, squids, and other fishes while at the same time supporting the diets of large predators such as tunas, sharks, and dolphins (Kiszka, Méndez-Fernandez, Heithaus, & Ridoux, 2014; Shimose & Wells, 2015; Torres-Rojas, Hernández-Herrera, Galván-Magaña, & Alatorre-Ramírez, 2010). This important family of fishes supports 5% of the annual marine finfish landings owing to its value as bait, sportfish, and food in many recreational and commercial fisheries (Ditty, Shaw, & Cope, 2004; Leak, 1981). Despite the importance of the Carangidae family, few studies have attempted to link oceanographic and environmental conditions to the distribution and abundance patterns of post-larvae and juvenile carangids in the oceanic GoM. Ditty et al. (2004) found carangid larvae were concentrated in areas of abundant zooplankton prey in the northern GoM, and suggested that dynamic frontal areas served as nurseries. Grimes and Finucane (1991) reported that carangids were the most abundant genera at the river plume and shelf-sampling stations in the northern GoM and hypothesized that increased feeding and growth would promote occupancy associated with river plume features. Carangids were also the most abundant species inside a river plume at the Great Barrier Reef, Australia (Thorrold & McKinnon, 1995). Given the sparse information on such an important epipelagic fish family in the GoM, the aim of the present study was to examine the role of oceanic conditions on the abundance and distribution of carangid fishes to better predict important areas such as spawning, nursery, and feeding grounds. In addition, conditions in the northern GoM in 2011 were influenced by natural gradients of salinity due to record freshwater discharge, providing an interesting setting in which to examine carangid responses. The objectives of this study were to (i) investigate carangid abundance and distribution in relation to sea surface temperature, salinity, and sea surface height anomaly in the GoM; (ii) compare the responses of post-larval and juvenile carangid life stages that were collected using two gear types across spring, summer and fall seasons; (iii) explore differences among the five most abundant carangid species collected. This information may provide important data for evaluating carangid responses to natural climate variability.

## 2 | METHODS

### 2.1 | Study area and collection methods

Collections occurred during four research cruise series totaling 160 days in the northern GoM in 2011: *Meg Skansi* A from 21 April–29 June ($N$ = 44 stations); *Meg Skansi* B from 20 July–28 September ($N$ = 44 stations); *Pisces* A from 23 June–12 July ($N$ = 12 stations); and *Pisces* B from 8 September–26 September ($N$ = 13 stations). These research expeditions were part of the larger Deepwater Horizon Natural Resource Damage Assessment (NRDA) conducted in the northern GoM (http://www.gulfspillrestoration.noaa.gov). Samples were collected aboard the R/V *Meg Skansi* using a 10-$m^2$ Multiple Opening and Closing Net and Environmental Sensing System (MOC) net (Wiebe et al., 1985; details below). The R/V *Pisces* deployed a large, dual-warp midwater trawl (LMT) net (Judkins, Vecchione,

Cook, & Sutton, 2016; details below). Fish abundance was standardized by dividing the number of fishes collected by the volume of water sampled ($m^3$) for each gear type. From here on each cruise will be identified by gear type deployed (MOC or LMT) and labeled by season. For instance, *Meg Skansi* A = MOC spring/summer; *Meg Skansi* B = MOC summer/fall; *Pisces* A = LMT summer; and *Pisces* B = LMT fall.

## 2.2 | R/V Meg Skansi: MOC sampling

A 10-$m^2$ mouth area MOC (3-mm mesh: MOC) net system was used owing to its capability of taking discrete samples over specific depth strata. At each station, a Conductivity, Temperature, and Depth (CTD) sensor array (SBE 911 Plus; Sea-Bird Electronics, Inc.) was cast at dawn and dusk. The MOC was deployed at either 09.00 or 21.00 hr such that either solar noon or midnight occurred at the midpoint of the tow. The MOC sampled from 0 to 1,500 m depth during descent and then sampled five depth strata discretely during retrieval: 1,500–1,200, 1,200–1,000, 1,000–600, 600–200, and 200–0 m. The volume filtered by each net was calculated using an algorithm that incorporated flowmeter (TSK model) data and net angle (inclinometer), with the latter used to estimate mouth area perpendicular to tow direction. Ship speed during net deployment was approximately 1.5 knots (1 knot = ~0.5 m/s). As a result of low numbers of carangid fishes collected in deep depth bins (Figure S1) only collections from the surface depth bin (0–200 m) were considered for further analysis. There was no significant difference in carangid abundance between day and night samples for MOC collections for all species pooled and individual species (Figure S2 and Table S1), thus day and night collections were pooled for each station to correspond with daily environmental measurements from the CTD and satellites.

## 2.3 | R/V Pisces: LMT sampling

The R/V *Pisces* conducted deep sampling using a large, dual-warp, high-speed pelagic trawl. The LMT is a commercial four-seam midwater trawl with a minimal drag that is capable of sampling larger and more mobile species than the MOC (Judkins et al., 2016). The mesh size of the LMT decreases along the body of the net from 6.5 m down to 6 cm at the last panel of webbing before the codend. Net mensuration sensors and data-loggers were used to actively monitor the fishing depth of the net during the tow. Data from these sensors also provided information on wingspread and mouth opening during the tow, which was then used to calculate approximate net geometry. The LMT effective mouth area was estimated to be 165.5 $m^2$. Volume filtered was calculated using an algorithm that incorporated mouth area and the oblique distance traveled by the net. Sampling occurred over a 24-hr period using oblique tows at a speed of five knots from the surface to depths ranging from 700 m to a maximum of 1,400 m. At each station, there were 2 day tows and two night tows; however, there was no significant difference in carangid abundance between day and night samples for LMT collections for all species pooled and individual species (Figure S3), thus day and night samples were pooled together for this study to correspond with daily environmental measurements from the CTD and satellites.

Once the nets were retrieved on deck, the catch was sorted into "rough" taxonomic groupings (i.e. fish families). Roughly sorted groupings were weighed on a motion-compensating scale and then preserved in 10% buffered formalin. All fishes from each station were kept and archived; nothing was discarded. Later sample processing in the laboratory involved further sorting, identification to lowest taxonomic level possible, species counts, cumulative species weights (wet weight, after blotting), and length measurements. Abundance data were standardized by effort (volume filtered, $m^3$). For the 10 $m^2$ MOC, volumes were calculated using flowmeter and net mouth angle data. The volume sampled using the LMT was two orders of magnitude larger compared to MOC cruises (Table 1); therefore, abundance was multiplied by 100,000 for MOC data (expressed as individuals [ind]/$m^3$ [$\times 10^{-5}$]) and by 10,000,000 for LMT data (ind/$m^3$ [$\times 10^{-7}$]) to make values comparable for plotting purposes by displaying abundances on similar scales. The spatial and seasonal distribution and abundance of carangid species were examined by generating contoured heat maps for each cruise using the Data-Interpolating Variational Analysis (DIVA: Troupin et al., 2012) gridding option in Ocean Data View (ODV version 4.5.6).

## 2.4 | Sample processing

All specimens collected in LMT and MOC samples were identified to the lowest possible taxonomic level, in most cases to the species

**TABLE 1** Summary statistics of mean (±*SD*) and range of physical factors measured with CTD (salinity), and satellite (SST and SSHA) at each station during each research cruise using the MOC and LMT during the spring, summer and fall of 2011

| | | Research cruise | | | |
|---|---|---|---|---|---|
| Physical factor | Statistic | MOC spring/summer | LMT summer | MOC summer/fall | LMT fall |
| Temperature (°C) | Mean | 26.9 ± 1.7 | 29.5 ± 0.43 | 30.5 ± 0.95 | 28.9 ± 2.2 |
| | Range | 24.4 to 29.7 | 29.1 to 30.5 | 28.6 to 31.8 | 27.7 to 29.5 |
| Salinity | Mean | 36 ± 1 | 34.5 ± 3.3 | 33.6 ± 2.7 | 35.3 ± 2.2 |
| | Range | 31.5 to 36.7 | 24.6 to 36.4 | 23 to 36.3 | 28.8 to 36.7 |
| SSHA (cm) | Mean | 6.6 ± 12.8 | 24.4 ± 15.6 | 16.4 ± 11 | 14.6 ± 10.8 |
| | Range | −11.5 to 42.3 | 3.7 to 46.7 | −0.36 to 48.7 | 3.7 to 38.5 |

level (93% of specimens). For groups that contained only a few specimens, all specimens were identified to the lowest taxonomic classification possible and measured to the nearest millimeter (mm) standard length (SL). For larger catches, a subset of 25 individuals were measured. The percent occurrence of each species was calculated as the number of stations a species was present divided by the total number of stations sampled.

## 2.5 | Environmental data

A CTD array was deployed at each site to record environmental variables including temperature, salinity, dissolved oxygen (DO) and fluorescence. DO and fluorescence data were not available for every site and therefore not included in further analysis. However, the limited fluorescence data was strongly correlated to salinity (Figure S4). Measurements from the upper 1–3 m and day and night were averaged together for daily measurements to correspond to daily satellite surface measurements. CTD salinity data were unavailable for 16% of the stations; therefore, the model estimated salinity data were used to fill in data gaps (explained below), and SST and SSHA was obtained exclusively from satellite data. SST measurements from the CTD were strongly correlated with remotely sensed SST values (Pearson's $r^2 = .92$, $p < .0001$, $N = 95$). Remotely sensed data for each station were obtained using the Marine Geospatial Ecology Tools (MGET) in ArcGIS (v10.2) (Roberts, Best, Dunn, Treml, & Halpin, 2010). SSHA measurements were obtained from Aviso DUAC 2014 gridded products from merged satellites at 1/3-degree resolution. SST estimates were gathered from the NASA JPL PO.DAAC MODIS Aqua satellites at 1/24-degree resolution. The HYCOM & NCODA models were used to estimate surface salinity at 1/25-degree resolution. All remotely sensed data from the LMT cruises were downloaded as mean statistics using cumulative climatology bins over the dates of each cruise that encompassed less than 2 weeks. For MOC cruise series that spanned over 3 months each, remotely sensed data were downloaded as mean statistics using a monthly climatological bin type. To examine the spatial and temporal variability in oceanographic conditions, surface layer maps of salinity (primarily measured with CTD), SST and SSHA (satellite measurements) were created in ODV (version 4.5.6) using the weighted average gridded data display option. The weighted average gridding option was chosen as it represents discreet values of conditions measured at each station where carangid abundance was quantified, and these paired measurements were used in GAM and RDA analysis.

## 2.6 | Statistical analysis

GAMs were used to explore relationships between carangid abundance (dependent variable) and physical oceanographic data, including salinity (CTD measurements), SST and SSHA (satellite measurements) as continuous explanatory variables and season as a categorical factor. GAMs are versions of Generalized Linear Models that permit complex nonlinear relationships between explanatory and response variables to be explored (Hastie & Tibshirani, 1986). Abundance estimates were rounded to the nearest integer for modeling purposes. The general GAM model follows the equation:

$$E[y] = g^{-1}\left(\beta_0 + \sum_k s_k(x_k)\right)$$

where $E[y]$ = the expected values of the response variable, $g$ = the link function, $\beta_0$ = the intercept, $x$ represents one of $k$ explanatory variables, and $s_k$ = the smoothing function for each explanatory variable.

Owing to the differences in size selectivity between MOC and LMT gear types, separate models were run for each dataset. Collinearity of explanatory variables was examined with variance inflation factors (VIF) in the *usdm* package in R version 3.0.2. The VIFs for all explanatory variables were ≤5 so all variables were used in the GAM models. Logarithmic links with cubic regression splines were fit with the software package *mgcv* in R. A negative binomial distribution was used because of the high abundance of zeros in the data set (Drexler & Ainsworth, 2013). All models employed four degrees of freedom for each variable to prevent over fitting and reduce the risk of generating ecologically unrealistic responses (Lehmann, Overton, & Leathwick, 2002). To explore potential effects of increased degrees of freedom, k was increased to 6, 8, and 10; however, the general shape of fish-environment relationships did not change. Response plots were generated for those physical variables that were deemed to have a significant influence ($\alpha = .05$) on the abundance of carangid fishes; non-significant variables were not plotted. To examine overall model fit, percent deviance explained (*DE*) was calculated for each model (([null deviance − residual deviance]/null deviance) × 100).

Ordination methods were used to further examine relationships between environmental conditions and the abundance of each species. Constrained linear Redundancy Analysis (RDA) was performed in CANOCO (version 5.04). The RDAs were run separately for each gear type to see if differences would be apparent between post-larval (MOC) and juvenile (LMT) life stages.

# 3 | RESULTS

## 3.1 | Oceanographic conditions

During MOC–spring/summer, the temperature was lower (25–26°C) in northern sites with negative (–10 to 0 cm) SSHA, but higher (>28°C) in southern central locations displaying positive (10–45 cm) SSHA (Figure 1a and e). The greatly increased SSHA (>30 cm) and increased temperature (>29°C) suggested an extension of the LC or an anticyclonic warm core eddy that traveled in a westerly direction between MOC–spring/summer and MOC–summer/fall (Figure 1e and f). Salinity was generally homogeneous (~36) during MOC–spring/summer except for a region of low salinity (~32) at a southern station with the highest SSHA (Figure 1c). Decreased salinities (24–32) were evident in northern regions of MOC–summer/fall

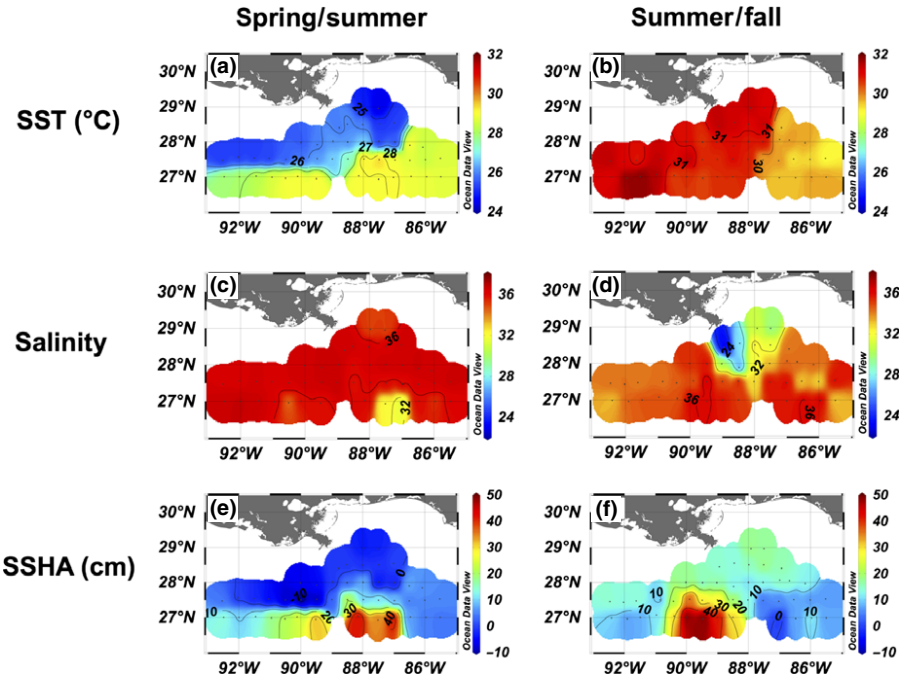


**FIGURE 1** Physical oceanographic conditions of temperature (SST) (a, b), salinity (c, d), and sea surface height anomaly (SSHA) (e, f) present during MOC sampling in the spring/early summer and late summer/fall of 2011. Colors represent weighted average gridding in ODV

indicating a southward extension of the Mississippi River plume (Figure 1d). During MOC–summer/fall, temperatures were approximately 5°C warmer compared with MOC–spring/summer in northern and western regions, but were ~2°C cooler in eastern regions that had displayed lower SSHA (Figure 1b and f). Similar patterns were exhibited during LMT–summer and LMT–fall cruises: lower salinities (26–32) in northern sites identified the river plume (Figure 2c and d) and positive SSHAs (35–45 cm) from the LC extension/anticyclonic eddy shifted in a westerly direction between the LMT–summer and LMT–fall (Figure 2e and f). For LMT–summer, warmer temperatures (30–31°C) occurred at the northern stations (Figure 2a), whereas for LMT–fall warmer temperatures (~30°C) were associated with positive SSHA (~35 cm) at western stations (Figure 2b and f). Descriptive statistics (mean ± standard deviation [*SD*]) and range for environmental data are presented amongst gear types and seasons (Table 1).

## 3.2 | Carangid abundance

A total of 8,436 carangid fishes were collected and identified to the family level or below (Table 2). The majority of carangids were collected during the LMT sampling, comprising 26% and 60% of the total catch in the summer and fall, respectively. Fewer carangids were collected during the MOC–summer/fall (12%) and MOC–spring/summer (2%) sampling. The two most abundant species were *Selene setapinnis* (34%) and *Caranx crysos* (30%), followed by *Caranx hippos* (10%), *Chloroscombrus chrysurus* (9%), and *Trachurus lathami* (8%). The genera *Caranx* (5%) and *Selene* (1%) were next in the order of the abundance, and these specimens were only identified to genera-specific taxonomic levels. Eleven additional species from the Carangidae family were also identified, but these comprised <2.8% of total abundance and thus were not included in the analysis owing to low sample sizes.

Carangid species displayed a higher frequency of occurrence in the LMT sampling compared to the MOC sampling (Table 3). For the LMT, *S. setapinnis*, *C. crysos*, *C. hippos*, and *T. lathami* all occurred in >75% of samples, whereas *C. chrysurus* occurred less frequently in only 26% of samples. Frequencies of occurrence of all carangid species from the MOC were generally low, ranging from 7%–35%, with *C. crysos* occurring most frequently (35%) and *C. chrysurus* occurring least frequently (7%) (Table 3). Length frequency histograms revealed that smaller carangids were collected during MOC compared with LMT (Figure 3). The median SL for MOC was 10 mm while the median SL for LMT was 23 mm. The range of carangid lengths overlapped between cruises (range MOC: 3–55 mm; range LMT: 9–149 mm), but larger fish were collected using the LMT (mean SL ± *SD* = 27.02 ± 15.94 mm) compared with the MOC (mean SL ± *SD* = 12.11 ± 6.62 mm) and this pattern was consistent for the top five most abundant species examined (Table 4).

## 3.3 | Carangid abundance and distribution

Carangid abundance heat maps were created for individual species and seasonal cruises to compare abundance and distribution throughout the northern GoM (Figures 4 and 5). For the MOC sampling *S. setapinnis* was absent in spring/summer except for 1 individual (Figure 4a), but in the summer/fall *S. setapinnis* displayed centralized high abundance (>60 ind/$m^3 \times 10^{-5}$) with zero abundance at western sites and increased abundance (~20 ind/$m^3 \times 10^{-5}$) at eastern sites (Figure 4b). Similarly, *C. crysos* abundance was low in the spring/summer in south-central sites and increased in the summer/fall with moderate abundance (20–40 ind/$m^3 \times 10^{-5}$) at single west and central sites, with higher abundance (20–80 ind/$m^3 \times 10^{-5}$) observed in the south eastern region (Figure 4c and d). *Caranx hippos* displayed low patchy abundance (2–4 ind/$m^3 \times 10^{-5}$) for MOC in the spring/summer in the central

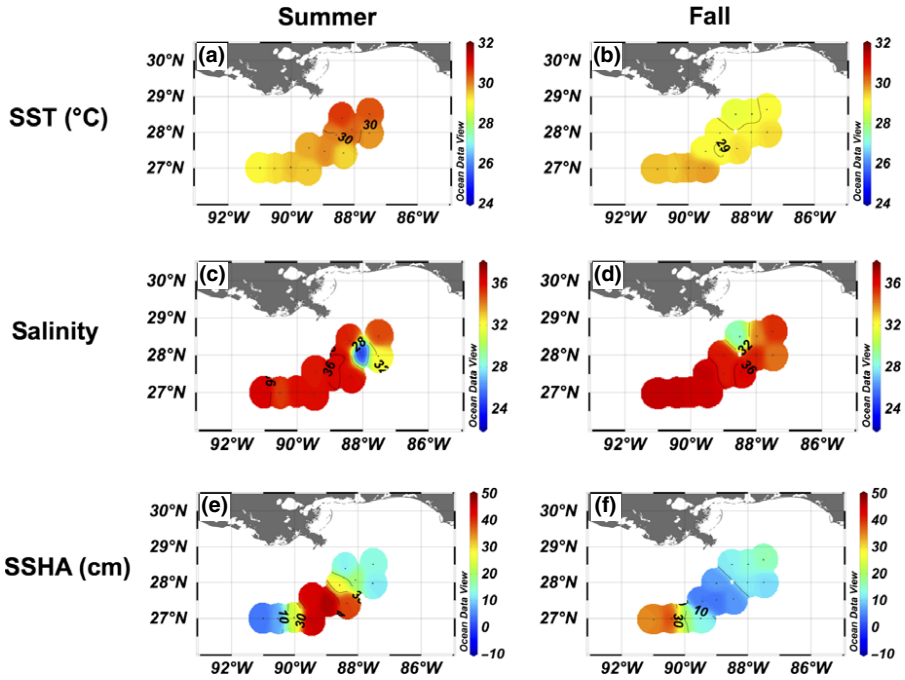


**FIGURE 2** Physical oceanographic conditions of temperature (SST) (a, b), salinity (c, d), and sea surface height anomaly (SSHA) (e, f) present during LMT sampling in the summer and fall of 2011. Colors represent weighted average gridding in ODV

**TABLE 2** Total numbers of carangid fishes (by genera and species) collected in the northern GoM using MOC and LMT gear types during the spring, summer and fall seasons. Total sum and average volume of water column sampled during each cruise also presented. Carangids listed highest to lowest based on total abundance. *Specimens only identified to the Genus level owing to morphological damage.

| | Research cruise | | | | |
|---|---|---|---|---|---|
| Species | MOC spring/summer | LMT summer | MOC summer/fall | LMT fall | Grand total |
| *Selene setapinnis* | 1 | 425 | 258 | 2,143 | 2,827 |
| *Caranx crysos* | 2 | 663 | 252 | 1,611 | 2,528 |
| *Caranx hippos* | 11 | 409 | 20 | 411 | 851 |
| *Chloroscombrus chrysurus* | | 130 | 357 | 254 | 741 |
| *Trachurus lathami* | 5 | 118 | 6 | 518 | 647 |
| *Caranx* sp.* | 96 | 314 | 42 | 8 | 460 |
| *Selene* sp.* | 30 | | 78 | 1 | 109 |
| *Caranx bartholomaei* | | 31 | 3 | 30 | 64 |
| *Selar crumenophthalmus* | 1 | 43 | 4 | 2 | 50 |
| *Decapterus* sp.* | 3 | 27 | | 10 | 40 |
| *Selene brownii* | | | | 36 | 36 |
| *Decapterus macarellus* | 15 | 12 | | 1 | 28 |
| *Decapterus tabl* | 6 | 12 | | 2 | 20 |
| *Caranx ruber* | | 12 | | | 12 |
| *Decapterus punctatus* | | | 9 | | 9 |
| *Alectis ciliaris* | | | 4 | 1 | 5 |
| *Selene vomer* | | 3 | 1 | | 4 |
| *Uraspis secunda* | | 3 | | 1 | 4 |
| *Pseudocaranx dentex* | | | 1 | | 1 |
| Grand total | 170 | 2,202 | 1,035 | 5,029 | 8,436 |
| Total sum of volume sampled | 1,378,606 | 110,127,577 | 1,927,156 | 113,497,582 | |
| Mean volume sampled | 49,236 | 9,177,298 | 52,085 | 8,730,583 | |

**TABLE 3** Frequency of occurrence for each of the most common carangid species collected using MOC and LMT gear

| | Carangid frequency of occurrence (%) | | | | | |
|---|---|---|---|---|---|---|
| Cruise | *Selene setapinnis* | *Caranx crysos* | *Caranx hippos* | *Chloroscombrus chrysurus* | *Trachurus lathami* | Species pooled |
| MOC | 26 | 35 | 10 | 7 | 8 | 70 |
| LMT | 76 | 88 | 76 | 28 | 76 | 100 |

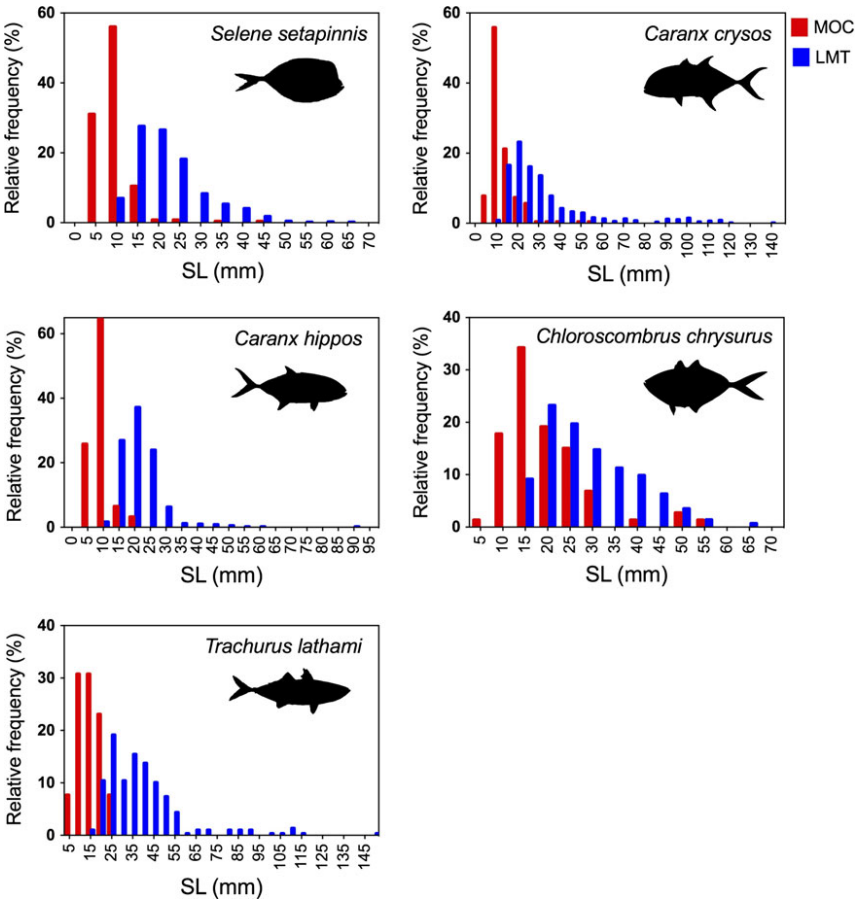


**FIGURE 3** Size frequency distribution for each carangid species collected using MOC (red) and LMT (blue) gear types

region and high abundance in the south eastern region during the summer/fall (Figure 4e and f). *Chloroscombrus chrysurus* was absent from spring/summer, but highly abundant (>300 ind/$m^3 \times 10^{-5}$) at one central station in the summer/fall (Figure 4g and h). *Trachurus lathami* exhibited low abundance (2–8 ind/$m^3 \times 10^{-5}$) that shifted from the east in the spring/summer to central and western sites in the summer/fall (Figure 4i and j).

For LMT carangid abundances were much higher in both the summer and fall compared to MOC (Figure 5). In the summer, *S. setapinnis* was most abundant (100–150 ind/$m^3 \times 10^{-7}$) in the north-central sites, but the abundances shifted to the east sites (400 ind/$m^3 \times 10^{-7}$) during the fall but abundances remained high in the north-central (200 ind/$m^3 \times 10^{-7}$) (Figure 5a and b). Abundances of *C. crysos* were increased (150 ind/$m^3 \times 10^{-7}$) at north-central sites in the summer and heavily concentrated (600 ind/$m^3 \times 10^{-7}$) at a single northern site in the fall (Figure 5c and d). *Caranx hippos* displayed high abundance (100 ind/$m^3 \times 10^{-7}$) at northern sites in the summer that shifted to western sites in the fall (Figure 5e and f). Abundances of *C. chrysurus* were increased (100 ind/$m^3 \times 10^{-7}$) at the northern site (Figure 5g and h) during both the summer and fall. *Trachurus lathami* exhibited moderate abundance (50 ind/$m^3 \times 10^{-7}$) at the northern site in the fall that increased and shifted to the west (200 ind/$m^3 \times 10^{-7}$) during the fall sampling (Figure 5i and j).

## 3.4 | Generalized additive models

Salinity was the only variable that exhibited a significant relationship to abundance for every carangid species (Table 5). However, those relationships varied among species and between gear types. In general, the deviance explained was high (*DE* > 50) for each species and gear type and ranged from 45% to 96% (Table 5). The season of collection was also a significant factor for most species, except for *C. chysurus* and *T. lathami* LMT collections (Table 5). *Selene setapinnis*

| Cruise | Species | N | Minimum | Maximum | Median | Mean ± SD |
|---|---|---|---|---|---|---|
| MOC | *Selene setapinnis* | 248 | 3 | 43 | 9 | 9.54 ± 3.98 |
| | *Caranx crysos* | 231 | 4 | 55 | 11 | 12.91 ± 6.55 |
| | *Caranx hippos* | 31 | 4 | 20 | 8 | 8.77 ± 2.98 |
| | *Chloroscombrus chrysurus* | 73 | 6 | 54 | 17 | 19.27 ± 8.97 |
| | *Trachurus lathami* | 13 | 6 | 24 | 16 | 14.54 ± 4.86 |
| | Combined | 596 | 3 | 55 | 10 | 12.11 ± 6.62 |
| LMT | *Selene setapinnis* | 1,104 | 9 | 66 | 20 | 22.15 ± 8.56 |
| | *Caranx crysos* | 949 | 10 | 142 | 26 | 32.27 ± 21.6 |
| | *Caranx hippos* | 605 | 11 | 92 | 21 | 21.31 ± 6.79 |
| | *Chloroscombrus chrysurus* | 142 | 13 | 67 | 27 | 29.21 ± 10.26 |
| | *Trachurus lathami* | 298 | 17 | 149 | 35 | 38.88 ± 18.89 |
| | Combined | 3,098 | 9 | 149 | 23 | 27.02 ± 15.94 |

*N*, sample size of measured fish; *SD*, standard deviation.
Size-frequency distribution presented in Figure 3.

**TABLE 4** Summary of standard length (SL) measurements (mm) for each carangid species collected using MOC of LMT gear

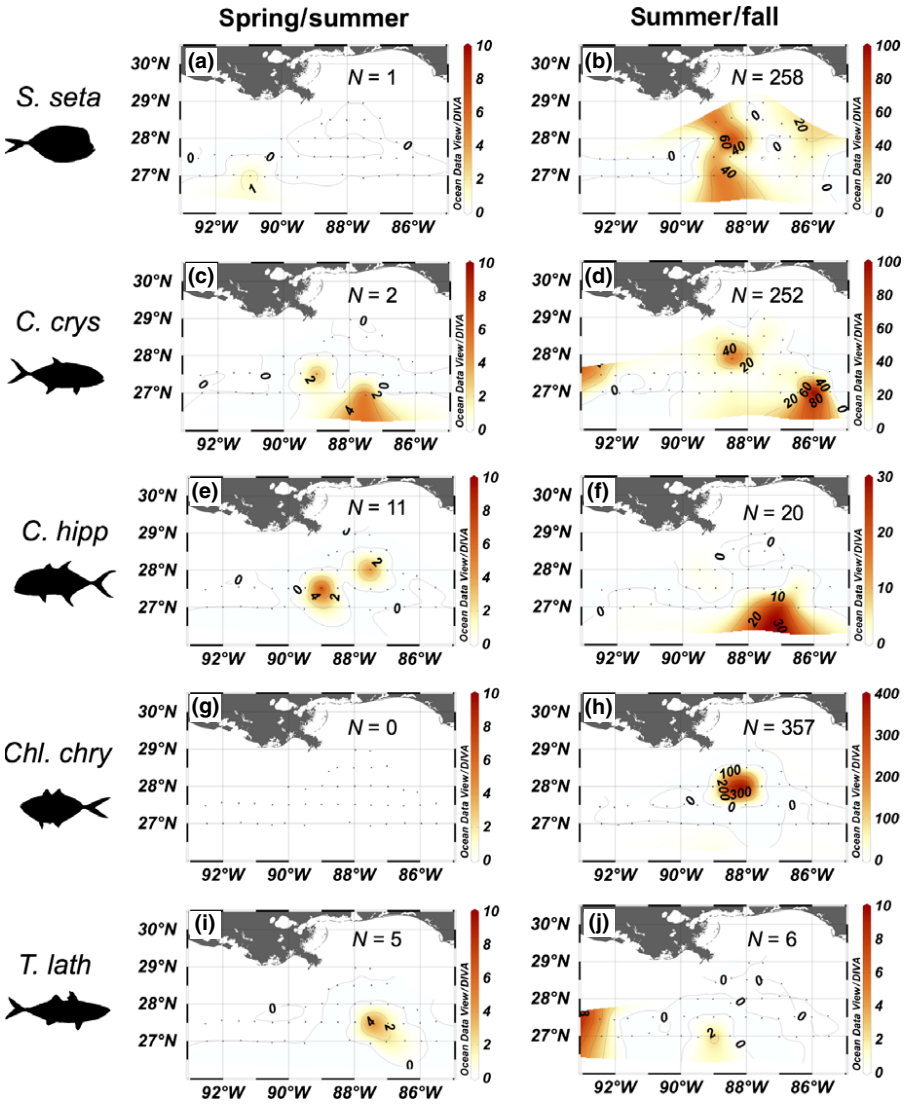


**FIGURE 4** Density distribution heat maps (ind/m$^3$ $10^{-5}$) for *Selene setapinnis* (a, b), *Caranx crysos* (c, d), *Caranx hippos* (e, f), *Chloroscombrus chrysurus* (g, h) and *Trachurus lathami* (i, j) collected during the MOC sampling in the spring/summer and summer/fall. Colors represent DIVA gridding in ODV; note difference in sample size (*N*) and scale bar for each plot

displayed increased abundance at high SSHA (>10 cm) and low salinities (<32) for MOC; however, the effect of temperature was not clear (Figure 6). For LMT, higher abundance of *S. setapinnis* was related to increased SST (>29.5°C) and decreased salinity with a dome-shaped peak at salinity = 29 (Figure 6). Salinity was the only factor significantly related to *C. crysos* abundance and the

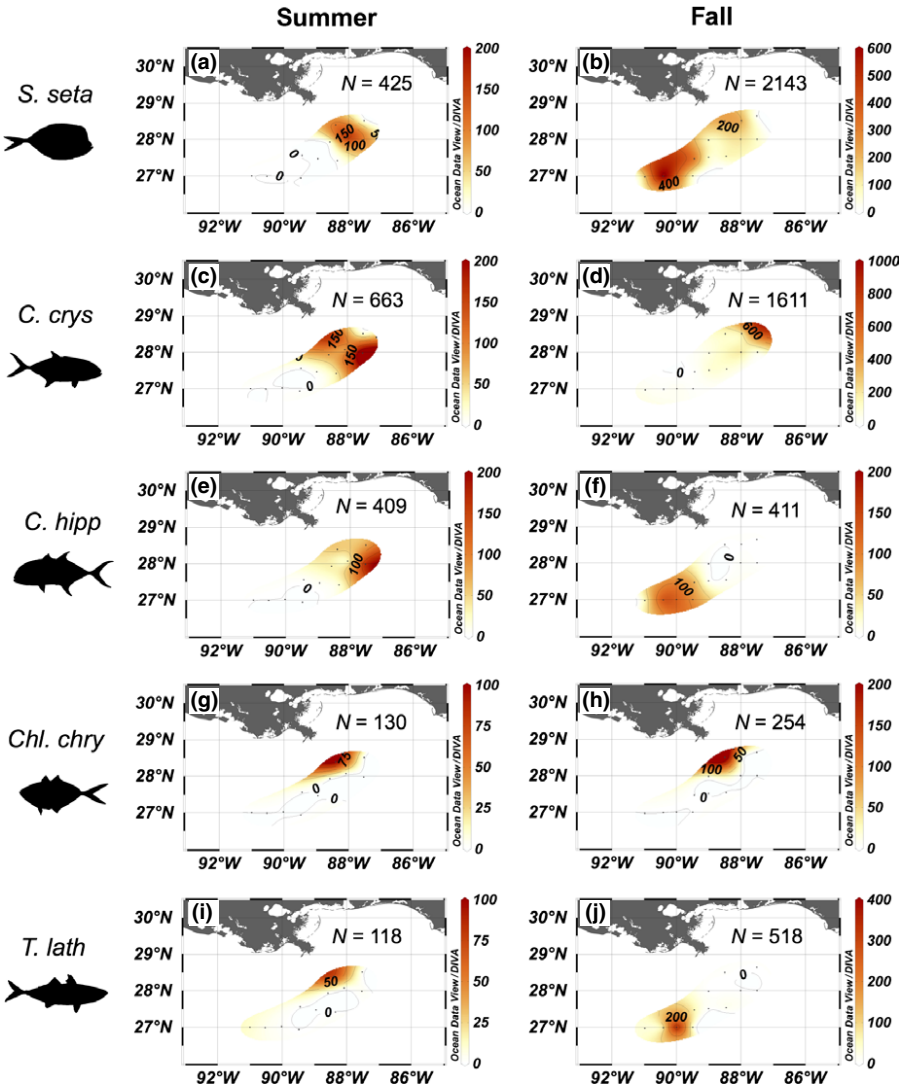


**FIGURE 5** Density distribution heat maps (ind/$m^3$ $10^{-7}$) for *Selene setapinnis* (a, b), *Caranx crysos* (c, d), *Caranx hippos* (e, f), *Chloroscombrus chrysurus* (g, h) and *Trachurus lathami* (i, j) collected during the LMT sampling in the summer and fall. Colors represent DIVA gridding in ODV; note difference in sample size (*N*) and scale bar for each plot

**TABLE 5** Generalized Additive Model (GAM) results demonstrating the influence of season and physical factors on the five most abundant carangid species collected during MOC and LMT sampling

| | | Factor | | | | |
|---|---|---|---|---|---|---|
| Cruise | Species | Season | SSHA | SST | Salinity | DE (%) |
| MOC | *Selene setapinnis* | **<0.0001** | **0.0005** | **<0.0001** | **<0.0001** | 69 |
| | *Caranx crysos* | **<0.0001** | 0.2191 | 0.0516 | **0.0092** | 53 |
| | *Caranx hippos* | **0.0007** | 0.0471 | **0.0092** | **0.0086** | 53 |
| | *Chloroscombrus chrysurus* | / | **0.0001** | **<0.0001** | **<0.0001** | 96 |
| | *Trachurus lathami* | **0.0007** | 0.1926 | **0.0064** | 0.5338 | 51 |
| LMT | *Selene setapinnis* | **<0.0001** | 0.1840 | **0.0000** | **<0.0001** | 63 |
| | *Caranx crysos* | **0.0001** | 0.0926 | 0.0745 | **0.0099** | 45 |
| | *Caranx hippos* | **0.0343** | 0.6130 | **0.0000** | **<0.0001** | 51 |
| | *Chloroscombrus chrysurus* | 0.2950 | 0.2322 | 0.1142 | **0.0322** | 95 |
| | *Trachurus lathami* | 0.0784 | **0.0002** | **0.0002** | **<0.0001** | 71 |

Significant variables ($p < .05$) in bold and percent deviance explained (DE) for each model is presented.

relationship shifted between MOC and LMT, with a peak at 27 for MOC and a peak at 32 for LMT (Figure 7). For MOC, higher *C. crysos* abundance occurred at salinities of 26–28, and for LMT there were higher abundances at salinities 30–34 (Figure 7). SST and salinity were significantly related to *C. hippos* abundance for both MOC and LMT, however, the shape and direction of the relationships differed between the gears (Figure 8). For MOC, higher *C. hippos* abundance was related to decreased SST (25–28°C) and

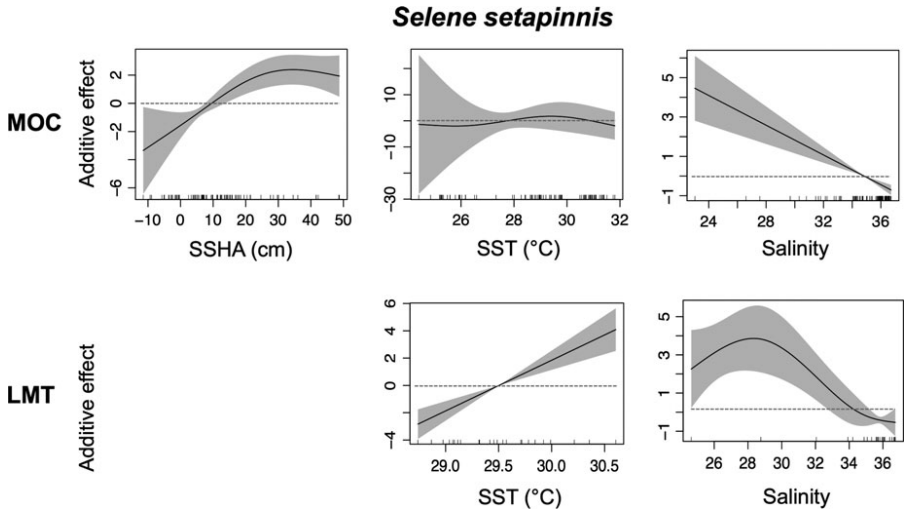


**FIGURE 6** Response plots for *Selene setapinnis* abundance in relation to sea surface temperature (SST), sea surface height anomaly (SSHA) and salinity determined from GAM models for fish collected using MOC and LMT. Non-significant variables not plotted

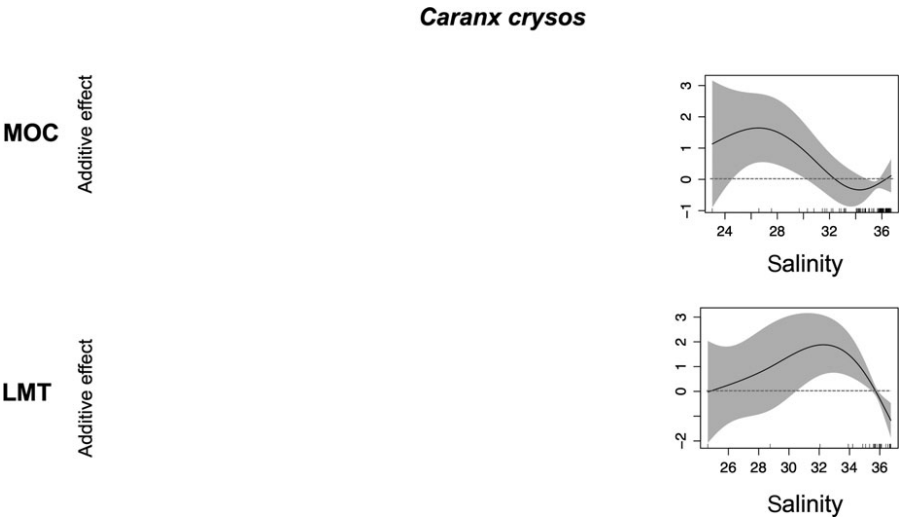


**FIGURE 7** Response plots for *Caranx crysos* abundance in relation to sea surface temperature (SST), sea surface height anolomy (SSHA) and salinity determined from GAM models for fish collected using MOC and LMT. Non-significant variables not plotted

increased salinity (>35) whereas for LMT there were more abundant *C. hippos* at increased SST (>29.5) and decreased salinity (26–32) (Figure 8). *Chloroscombrus chrysurus* collected with MOC exhibited increased abundance at decreased SSHA (<5 cm), decreased salinity (26–30), and increased SST (>28°C), whereas *C. chysurus* collected with LMT was more abundant at low salinities (<35) (Figure 9). For both MOC and LMT, increased *T. lathami* abundance was significantly related to increased SST (Figure 10). For LMT, the response of *T. lathami* to salinity was variable, with increased abundance observed at moderate (27–30) and higher (>35) salinities (Figure 10). The abundance of *T. lathami* was increased at moderate SSHA (0–20 cm) for LMT (Figure 10).

Environmental variables accounted for 27% and 20.1% of the variation in species for MOC and LMT, respectively (Figure 11). The RDA plots demonstrated that *S. setapinnis*, *C. crysos* and *C. chrysurus* all responded similarly with increased abundance at low salinities for both post-larval (Figure 11a) and juvenile (Figure 11b) life stages. However, the post-larval stage of *S. setapinnis*, *C. crysos* and *C. chrysurus* were more abundant at higher temperatures, whereas the juvenile stages were more abundant at lower SSHA (Figure 11). *Caranx hippos* and *T. lathami* displayed similar spatial arrangement in RDA plots for both post-larval and juvenile life stages, with higher abundances at higher SST (Figure 11a and b).

## 4 | DISCUSSION

The northern GoM in 2011 displayed sharp gradients of SST, salinity, and SSHA, which affected the abundance and distribution of post-larval and juvenile carangids. Lower salinities that are characteristic of the Mississippi River plume tended to result in increased abundance of most carangids, but responses to SST and SSHA were species- and life-stage specific. The seasonal sampling that encompassed the spring, summer and fall captured many gradients in oceanographic conditions that represent dominant mesoscale features in the GoM including the river plume, warm core eddies and/or the extension of the LC, and frontal regions where the eddies and the plume intersect. Additionally, the use of two gear types with different mesh size and tow speeds allowed comparison between abundance and distribution of post-larval and juvenile carangid species life stages.

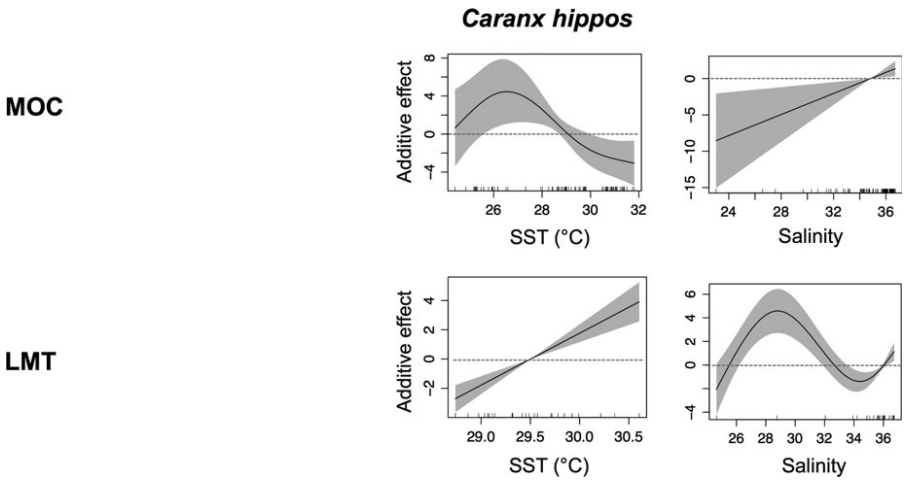


**FIGURE 8** Response plots for *Caranx hippos* abundance in relation to sea surface temperature (SST), sea surface height anolomy (SSHA) and salinity determined from GAM models for fish collected using MOC and LMT. Non-significant variables not plotted

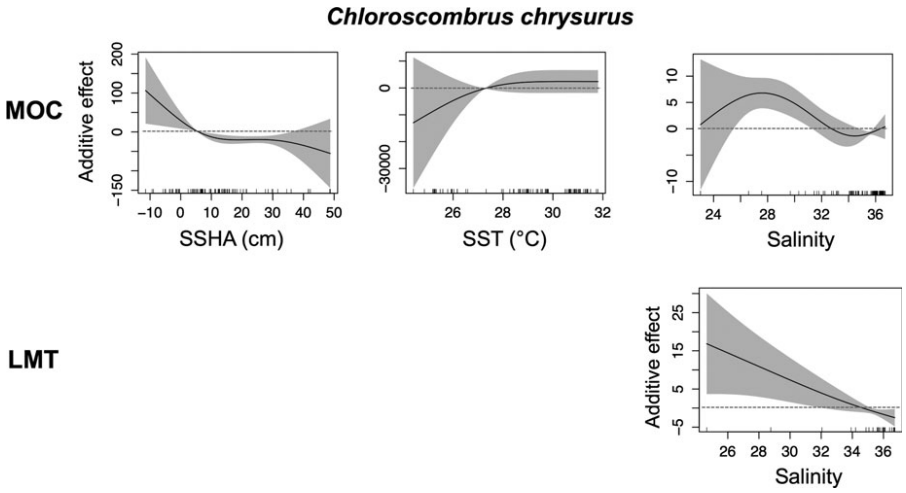


**FIGURE 9** Response plots for *Chloroscombrus chrysos* abundance in relation to sea surface temperature (SST), sea surface height anolomy (SSHA) and salinity determined from GAM models for fish collected using MOC and LMT. Non-significant variables not plotted

Many of the studies that have examined the influence of abiotic factors on the distribution and abundance of marine fishes in the GoM have focused on larval life stages (Kitchens & Rooker, 2014; Randall, Smith, Cowan, & Rooker, 2015; Rooker et al., 2012). Larvae exhibit limited mobility and are easy to collect in towed nets. Additionally, collecting larvae allows inference on spawning location and season (Ditty et al., 2004; Kitchens & Rooker, 2014; Rooker et al., 2012; Shaw & Drullinger, 1990). Fewer studies have focused on juvenile and sub-adult life stages of marine fishes, potentially owing to the high mobility of juvenile life stages and net avoidance behavior (Leak, 1981). Smaller carangids were collected during MOC sampling with small mesh size (3 mm) resulting in a median fish SL of 10 mm, a size suggesting these fishes were post-larvae in a transitory phase between larvae and juvenile life stages (Aprieto, 1974). Larger juvenile and sub-adult fishes with a median SL of 23 mm were collected in LMT that utilized the larger mesh size (51 mm) with a 16.5× greater effective mouth area; however, both net styles did collect some carangids that were larger than 50 mm, but these subadult/adult specimens were rare. Larger carangids were collected in the LMT owing to faster tow speeds of 2.6 m/s compared to the MOC, which towed at speeds of 0.8 m/s. Leis, Hay, Clark, Chen, and Shao (2006) calculated in situ swimming speeds in larvae and early juvenile (8–18 mm SL) of a related carangid, the Giant Trevally *Caranx ignobilis*, and determined swimming speeds ranged from 2 to 20 cm/s that was linearly related to SL. Therefore, applying the linear size-to-swimming speed relationship of Leis et al. (2006), a carangid juvenile of SL = 50 mm could swim approximately 70 cm/s, or near the tow speed of the MOC net and a 100-mm juvenile would approach speeds of 140 cm/s. Larger carangids most likely escaped net capture by swimming faster than the net tow speed or moving vertically or horizontally in the water column to avoid the approach of the net (Misund, Luyeye, Coetzee, & Boyer, 1999). Although larval and juvenile carangids prefer pelagic habitats, some adult carangids prefer benthic habitats (Clarke & Aeby, 1998) and thus adults may not have been targeted by the gear types used here. Most of the carangid species examined here spawn in neritic coastal waters, where most previous surveys have focused sampling effort in shallow water <100 m deep (Espinosa-Fuentes & Flores-Coto, 2004; Katsuragawa & Ekau, 2003; Leak, 1981; Shaw & Drullinger, 1990). In contrast, samples in this study were collected far offshore in depths ranging from 500 to 3,000 m. Thus, the gear types used here and areas sampled most likely captured late stage larvae to early/late juveniles that were

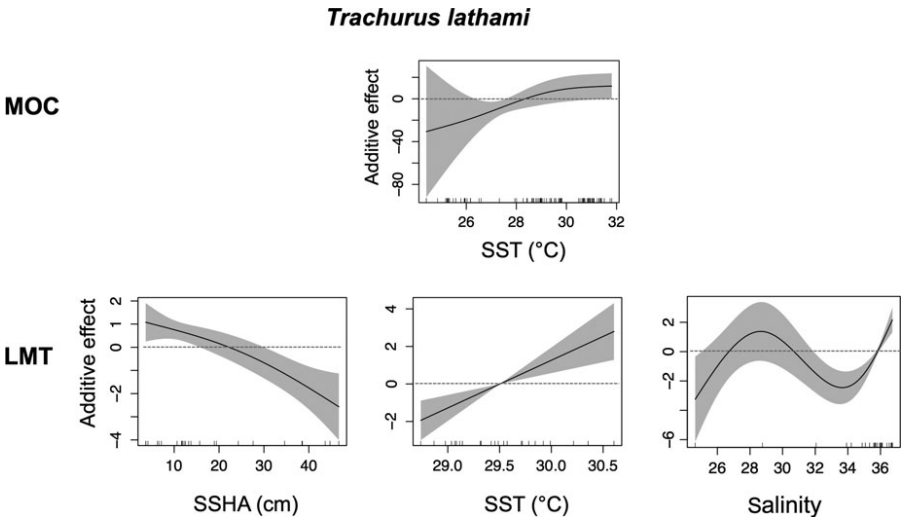


**FIGURE 10** Response plots for *Trachurus lathami* abundance in relation to sea surface temperature (SST), sea surface height anolomy (SSHA) and salinity determined from GAM models for fish collected using MOC and LMT. Non-significant variables not plotted

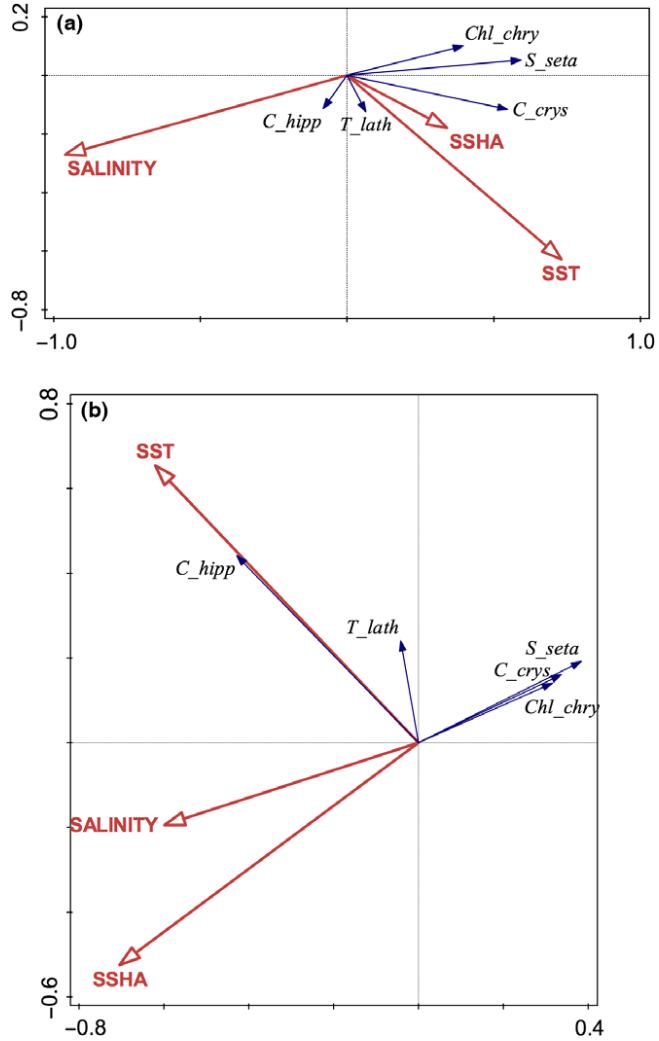


**FIGURE 11** Redundancy analysis (RDA) plots exploring relationships between environmental factors (red arrows) and species abundance (weighted average = triangles) for MOC (a) and LMT (b) collected samples

either passively entrained in circulation patterns of the expansive river plume (Grimes & Finucane, 1991; Johns et al., 2014) or actively engaging in ontogenetic migrations from nearshore to offshore habitats (da Costa, Albieri, & Araújo, 2005) or aggregating in the hydrodynamic nutrient rich and productive frontal regions (Ditty et al., 2004; Raya & Sabates, 2015).

## 4.1 | Abundance ranking among species

The two most abundant species collected in this study were the *S. setapinnis* (34%) and *C. crysos* (30%), which together comprised 64% of all species collected. Few studies have reported a high abundance of *S. setapinnis*, ranging from 0.2% to 2% of collections in the southern Atlantic off the Brazilian coast (Campos, De Castro, & Bonecker, 2010; de Souza & Junior, 2008). Flores-Coto and Sanchez-Ramirez (1989) found *S. setapinnis* comprised 6.1% of collections and were most abundant in warmer months in the southern GoM, which was the highest reported abundance of *S. setapinnis* before this study. This is in contrast with results of other studies in the GoM, which have typically found *C. chrysurus* to be the dominant species (Ditty et al., 2004; Flores-Coto & Sanchez-Ramirez, 1989). da Costa et al. (2005) examined carangid distributions in a semi-enclosed bay in southeastern Brazil and found *C. chrysurus* abundance and biomass was significantly related to decreased salinity and shallow water depths. This relationship was the result of a high number of juveniles (30–90 mm total length) collected from the inner bay which exhibited increased water temperature, low water clarity, and high organic loads that supported increased primary production and upper trophic levels (da Costa et al., 2005). Ditty et al. (2004) sampled carangid larvae in the northern GoM and reported abundance rankings of: *C. chrysurus* 83%; *Decapterus punctatus* 9%; *C. hippos* 2.9%; *C. crysos* 1.9%. *Chloroscombrus chrysurus* was most abundant west of the Mississippi River, whereas *D. punctatus* was most abundant in the eastern GoM on the Florida Shelf. *Caranx hippos* and *C. crysos* had similar spatial overlap, but different temporal distributions with *C. hippos* more abundant in May-June whereas *C. crysos* occurred more frequently in June to August (Ditty et al., 2004). Interestingly, we found different salinity preferences for both post-larval and juvenile *C. crysos* and *C. hippos*, suggesting spatial separation and habitat partitioning between these species. Leak

(1981) sampled carangid larvae in the eastern GoM during 4 years and found that *D. punctatus* were over 10× more abundant than all other carangids. Shaw and Drullinger (1990) sampled carangid larvae in coastal waters of Louisiana during 1982–83 and found *C. chrysurus* was most abundant followed by *C. crysos*, *T. lathami*, and *D. punctatus* in order of abundance. In the southern GoM below 21°N, Flores-Coto and Sanchez-Ramirez (1989) examined seasonal carangid densities in 1983–84 and described ranked abundance of the same species examined here: *C. chrysurus* 54%; *D. punctatus* 16%; *T. lathami* 12%; *S. setapinnis* 6%; *C. hippos* 0.9% and *C. crysos* 0.7%. Larvae of these carangids were present year-round, except for *T. lathami*, which was only present in the winter and spring. Several other studies have been conducted off the Brazilian coast and have found different patterns of carangid abundance (Campos et al., 2010; de Souza & Junior, 2008; Katsuragawa & Matsuura, 1992). Katsuragawa and Matsuura (1992) reported abundances of *T. lathami* 59%; *C. chrysurus* 15%; *D. punctatus* 12%, whereas Campos et al. (2010) reported abundances of *Decapterus puntatus* 57%; *C. chrysurus* 17%; *C. crysos* 8%, *T. lathami* 6% and *S. setapinnis* 0.2%, which was similar to the findings of de Souza and Junior (2008). The primary difference between previous work and this study was the high density of the *S. setapinnis* exhibited here, and the lack of *D. puntatus* that is typically a highly abundant carangid in the GoM and South Atlantic Ocean. *Decapterus puntatus* spawn year-round in the eastern GoM and display more intense spawning at higher temperatures (26–32°C) and increased salinities (36–37) and perhaps were less abundant in the low salinity conditions of 2011 compared to other carangid species (Leak, 1981). *Decapterus puntatus* are also more concentrated in the eastern GoM on the Florida shelf (Ditty et al., 2004; Leak, 1981) in an area that was not sampled in this study. Shaw and Drullinger (1990) sampled carangid larvae in coastal waters of Louisiana and found *T. lathami* was restricted to deeper depths (the mean depth range 221–2,768 m) and high salinities (mean salinity 36). Spawning of *T. lathami* is known to be associated with "high amplitude event or gradients" and larvae have been collected from turbulent mixed water between the river plume and oceanic waters (Shaw & Drullinger, 1990). Although *T. lathami* were found offshore in agreement with other studies, *T. lathami* presence in warmer waters has not been reported previously.

## 4.2 | Inferred spawning seasons and habitats

The MOC collected post-larval carangids, which displayed consistent and narrow size ranges indicated by median SL from 8 to 17 mm. Most of the post-larval carangids displayed low abundance from the spring/summer samples collected in April and June, except for *T. lathami* which had comparable abundances between the seasons but different distributions. *Trachurus lathami* is the only species thought to spawn in the winter, whereas all the other species spawn in the summer, which would explain the higher abundance of *S. setapinnis, C. crysos, and C. chrysurus* in the summer and fall seasons (Ditty et al., 2004; Leak, 1981; Shaw & Drullinger, 1990). The post-larval abundances of three species (*S. setapinnis*, *C. chrysurus*, and *T. lathami*) displayed complex relationships with SST. In general, there were higher abundances at increased temperatures (also evident in the RDA plot), but there was high variability in the GAM response plots resulting in funnel shaped curves at lower temperatures. In contrast, *C. hippos* post-larvae displayed a distinct peak at lower temperatures (25–28°C) and low abundance at high temperatures. *Caranx hippos* was also the only species that demonstrated increased abundance at high salinities >35. These results suggest a separation of spawning habitat between *C. hippos* and the other carangids examined here. *Caranx hippos* was also the only species that displayed contrasting relationships between abundance and SST and salinity between post-larvae and juveniles. Additionally, the non-overlapping spatial distributions and different shapes of the salinity response plot among species may suggest a temporal or spatial succession of spawning events to reduce inter-species competition for resources (Raya & Sabates, 2015). For instance, *S. setapinnis* displayed a linear salinity response plot, whereas *C. crysos* and *C. chrysurus* were domed shaped and *C. hippos* was linear but negative. Species-specific responses of post-larvae abundance to SSHA were also detected. *Chloroscombrus chrysurus* abundance was increased at lower SSHA, whereas *S. setapinnis* was more abundant at increased SSHA, providing further evidence of habitat partitioning between species. A study of billfish spawning habitats in the northern GoM found higher densities of sailfish and swordfish larvae at low SSHA (<10 cm), but blue marlin larvae displayed increased density at high (>20 cm) and low SSHA (<−5 cm) (Rooker et al., 2012). Randall et al. (2015) reported increased bluntnose flyingfish *Prognichthys occidentalis* larvae at low SSHA (<0 cm) and high salinity (>35) and suggested the expansive river plume in 2011 may have decreased suitable spawning habitat for *P. occidentalis*, in contrast to our findings for carangids.

The commonalities and differences in species-environment relationships were also exhibited in the RDA ordination plots, where *S. setapinnis*, *C. crysos*, and *C. chrysurus* were correlated positively with SST and SSHA, and negatively correlated with salinity whereas *C. hippos* was opposite of those three species. Other studies have demonstrated that river plume features can be characterized by low salinity and increased temperature (Johns et al., 2014). The higher abundance of *S. setapinnis*, *C. crysos*, and *C. chrysurus* post larvae at lower salinities and warmer SST suggests association with the river plume that could either result from passive entrainment of small buoyant larvae due to hydrodynamic convergence zones (Bakun, 2006; Govoni, Hoss, & Colby, 1989) or active seeking out of plume waters for feeding (Govoni & Chester, 1990). Enhanced larval feeding may result from the photic environment of the plume, where increased suspended sediments may increase the visual contrast and overall diversity of prey types (Govoni & Chester, 1990). Dagg and Whitledge (1991) reported strong seasonality of zooplankton production in the MS River plume, with highest production occurring in the summer which concurs with our results of higher larval concentrations in the summer/fall compared to the spring/summer MOC cruises. Increased abundance of larval fishes at productive frontal zones would also attract predators, which could explain the higher

occurrence of juvenile and larger carangid collected with LMT in the plume and or frontal zones. Thus, perhaps some larger sized carangids (>40 mm) were inhabiting the river plume to forage on other smaller larval fish that may be entrained passively in the plume.

Juvenile carangids collected with LMT experienced a much narrower SST range (27.7–30.5°C) compared with the larval MOC SST range (24.4–31.8), which may explain the consistent linear relationship between juvenile abundance and SST for *S. setapinnis*, *C. hippos* and *T. lathami*. However, SST was not significantly related to *C. chrysurus* and *C. crysos* juvenile abundance. Interestingly, on the RDA plot only *C. hippos* and to a lesser extent *T. lathami* showed directional ordination with SST. Similar to the post-larval carangids, higher abundances of juvenile carangids were generally found at lower salinities and salinity was a significant variable in the GAM models for all juvenile (LMT) carangids. However, the GAM response plots were linear for *C. chrysurus*, dome-shaped for *S. setapinnis* and *C. crysos*, and S-shaped for *C. hippos* and *T. lathami*, suggesting increased abundance at both medium and high salinities. This difference was also apparent in the RDA plot, where *C. hippos* and *T. lathami* pointed in different directions than the other species, suggesting habitat partitioning between the species. The abundance heat map also identified a unique seasonal pattern for *C. hippos* and *T. lathami* (and to a lesser extent *S. setapinnis*) where the distribution shifted from the northern region in the summer to more western regions in the fall. Perhaps the westerly shifts in abundance were related to the westerly moving warm core eddy/LC extension that produced a frontal region with increased production and food availability at the intersection of the mesoscale eddy and river plume. In contrast, to the post-larval carangids that may have been passively entrained in the frontal convergence zones, it is likely the larger juveniles targeted frontal zones for increased feeding (Bakun, 2006). Additionally, the schooling behavior of carangid juveniles may have resulted in patchy concentrated zones (Kwei, 1978) that were evident from highly localized abundance exhibited on the species heat maps.

## 5 | CONCLUSION

Relationships between carangid abundance and physical oceanographic features were examined in the northern GoM in 2011, when the Mississippi River experienced record flooding. MOC and LMT gear types were used to collect fish and both in situ CTD and satellite measurements were used to characterize physical conditions and mesoscale features. SST, salinity, and SSHA, were related to carangid density and varied between species as a product of differences in life history strategies between post-larval and juveniles. The large expansion of the Mississippi River plume in the record-flooding year, created frontal zones with dynamic salinity and temperature regimes that may have passively entrained post-larval carangids or aggregated foraging juveniles. Additional future studies may focus on growth measurements via otolith microstructure analyses and dietary analysis with stomach contents and tissue stable isotope analyses (Syahailatua, Taylor, & Suthers, 2011) to examine potential resource partitioning between species over multiple years.

## ACKNOWLEDGEMENTS

This manuscript includes both work that was conducted and samples that were collected as part of the Deepwater Horizon Natural Resource Damage Assessment being conducted cooperatively among academic partners, NOAA, other Federal and State Trustees, and BP. This research was made possible in part by a grant from The Gulf of Mexico Research Initiative. Data are publicly available through the Gulf of Mexico Research Initiative Information & Data Cooperative (GRIIDC) at https://data.gulfresearchinitiative.org (doi: 10.7266/N7VX0DK2, 10.7266/N7R49NTN). The findings and conclusions in this manuscript are those of the authors and do not necessarily represent the view of the National Oceanic and Atmospheric Administration or of any other natural resource trustee for the BP/Deepwater Horizon Natural Resource Damage Assessment. This is contribution #35 from the Marine Education and Research Center in the Institute for Water and Environment at Florida International University.

## REFERENCES

Aprieto, V. L. (1974). Early development of five Carangid fishes of the Gulf of Mexico and the south Atlantic coast on the United States. *Fishery Bulletin*, *72*, 415–443.

Bakun, A. (2006). Fronts and eddies as key structures in the habitat of marine fish larvae: Opportunity, adaptive response and competitive advantage. *Scientia Marina*, *70*(S2), 105–122.

Biggs, D. (1992). Nutrients, plankton, and productivity in a awarm-core ring in the western Gulf of Mexico. *Journal of Geophysical Research*, *97*, 160–163.

Biggs, D. C., & Müller-Karger, F. E. (1994). Ship and satellite observations of chlorophyll stocks in interacting cyclone-anticyclone eddy pairs in the western Gulf of Mexico. *Journal of Geophysical Research: Oceans*, *99*, 7371–7384.

Campos, P. N., De Castro, M. S., & Bonecker, A. C. T. (2010). Occurrence and distribution of Carangidae larvae (Teleostei, Perciformes) from the Southwest Atlantic Ocean, Brazil (12-23oS). *Journal of Applied Ichthyology*, *26*, 920–924.

Chesney, E., Baltz, D., & Thomas, R. (2000). Louisiana estuarine and coastal fisheries and habitats: Perspectives from a fish's eye view. *Ecological Applications*, *10*, 350–366.

Clarke, T. A., & Aeby, G. S. (1998). The use of small mid-water attraction devices for investigation of the pelagic juveniles of carangid fishes in Kaneohe Bay, Hawaii. *Bulletin of Marine Science*, *62*, 947–955.

da Costa, M. R., Albieri, R. J., & Araújo, F. G. (2005). Size distribuition of the jack *Chloroscombrus chrysurus* (Linnaeus) (Actinopterygii, Carangidae) in a tropical bay at southeastern Brazil. *Revista Brasileira de Zoologia*, *22*, 580–586.

Dagg, M. J., & Breed, G. A. (2003). Biological effects of Mississippi River nitrogen on the northern Gulf of Mexico – A review and synthesis. *Journal of Marine Systems*, *43*, 133–152.

Dagg, M. J., & Whitledge, T. E. (1991). Concentrations of copepod nauplii associated with the nutrient-rich plume of the Mississippi River. *Continental Shelf Research*, *11*, 1409–1423.

de Souza, C. S., & Junior, P. M. (2008). Distribution and abundance of Carangidae (Teleostei, Perciformes) associated with oceanographic factors along the Northeast Brazilian Exclusive Economic Zone. *Brazilian Archives of Biology and Technology*, *51*, 1267–1278.

Del Castillo, C. E., Coble, P. G., Conmy, R. N., Müller-Karger, F. E., Vanderbloemen, L., & Vargo, G. A. (2001). Multispectral in situ measurements of organic matter and chlorophyll fluorescence in seawater: Documenting the intrusion of the Mississippi River plume in the West Florida Shelf. *Limnology and Oceanography*, *46*, 1836–1843.

Ditty, J. G., Shaw, R. F., & Cope, J. S. (2004). Distribution of carangid larvae (Teleostei: Carangidae) and concentrations of zooplankton in the northern Gulf of Mexico, with illustrations of early *Hemicaranx amblyrhynchus* and *Caranx* spp. larvae. *Marine Biology*, *145*, 1001–1014.

Drexler, M., & Ainsworth, C. H. (2013). Generalized additive models used to predict species abundance in the Gulf of Mexico: An ecosystem modeling tool. *PLoS One*, *8*, e64458.

Espinosa-Fuentes, M. L., & Flores-Coto, C. (2004). Cross-shelf and vertical structure of ichthyoplankton assemblages in continental shelf waters of the Southern Gulf of Mexico. *Estuarine, Coastal and Shelf Science*, *59*, 333–352.

Falcini, F., Khan, N. S., Macelloni, L., Horton, B. P., Lutken, C. B., McKee, K. L. … Jerolmack, D. J. (2012). Linking the historic 2011 Mississippi River flood to coastal wetland sedimentation. *Nature Geoscience*, *5*, 803–807.

Flores-Coto, C., & Sanchez-Ramirez, M. (1989). Larval distribution and abundance of Carangidae (Pisces), from the southern Gulf of Mexico. 1983–1984. *Gulf and Caribbean Research*, *8*, 117–128.

Gierach, M. M., Vazquez-Cuervo, J., Lee, T., & Tsontos, V. M. (2013). Aquarius and SMOS detect effects of an extreme Mississippi River flooding event in the Gulf of Mexico. *Geophysical Research Letters*, *40*, 5188–5193.

Godø, O. R., Samuelsen, A., Macaulay, G. J., et al. (2012). Mesoscale eddies are oases for higher trophic marine life. *PLoS One*, *7*, e30161.

Govoni, J., & Chester, A. (1990). Diet composition of larval *Leistomus xanthurus* in and about the Mississippi River plume. *Journal of Plankton Research*, *12*, 819–830.

Govoni, J. J., Hoss, D. E., & Colby, D. R. (1989). The spatial distribution of larval fishes about the Mississippi River plume. *Limnology and Oceanography*, *34*, 178–187.

Grimes, C. (2001). Fishery production and the Mississippi River discharge. *Fisheries*, *26*, 17–26.

Grimes, C., & Finucane, J. (1991). Spatial distribution and abundance of larval and juvenile fish, chlorophyll and macrozooplankton around the Mississippi River discharge plume, and the role of the plume in fish recruitment. *Marine Ecology Progress Series*, *75*, 109–119.

Hamilton, P. (1992). Lower continental slope cyclonic eddies in the central Gulf of Mexico. *Journal of Geophysical Research*, *97*, 2185–2220.

Hastie, T. J., & Tibshirani, R. (1986). Generalized additive models. *Statistical Science*, *1*, 297–318.

Johns, E. M., Muhling, B. A., Perez, R. C., et al. (2014). Amazon River water in the northeastern Caribbean Sea and its effect on larval reef fish assemblages during April 2009. *Fisheries Oceanography*, *23*, 472–494.

Judkins, H., Vecchione, M., Cook, A., & Sutton, T. (2016). Diversity of midwater cephalopods in the northern Gulf of Mexico: Comparison of two collecting methods. *Marine Biodiversity*, 1–11. http://link.springer.com/article/10.1007/s12526-016-0597-8.

Katsuragawa, M., & Ekau, W. (2003). Distribution, growth and mortality of young rough scad, *Trachurus lathami*, in the south-eastern Brazilian Bight. *Journal of Applied Ichthyology*, *19*, 21–28.

Katsuragawa, M., & Matsuura, Y. (1992). Distribution and abundance of carangid larvae in the southeastern Brazilian Bight during 1975–1981. *Boletim do Instituto Oceanográfico*, *40*, 55–78.

Kiszka, J. J., Méndez-Fernandez, P., Heithaus, M. R., & Ridoux, V. (2014). The foraging ecology of coastal bottlenose dolphins based on stable isotope mixing models and behavioural sampling. *Marine Biology*, *161*, 953–961.

Kitchens, L. L., & Rooker, J. R. (2014). Habitat associations of dolphinfish larvae in the Gulf of Mexico. *Fisheries Oceanography*, *23*, 460–471.

Kwei, E. A. (1978). Food and spawning activity of *Caranx hippos* off the coast of Ghana. *Journal of Natural History*, *12*, 195–215.

Leak, J. C. (1981). Distribution and abundance of Carangid fish larvae in the Eastern Gulf of Mexico, 1971–1974. *Biological Oceanography*, *1*, 1–28.

Lehmann, A., Overton, J. M. C., & Leathwick, J. R. (2002). GRASP: Generalized regression analysis and spatial prediction. *Ecological Modelling*, *157*, 189–207.

Leis, J. M., Hay, A. C., Clark, D. L., Chen, I. S., & Shao, K. T. (2006). Behavioral ontogeny in larvae and early juveniles of the giant trevally (*Caranx ignobilis*) (Pisces: Carangidae). *Fishery Bulletin*, *104*, 401–414.

Lima, I. D., Olson, D. B., & Doney, S. C. (2002). Biological response to frontal dynamics and mesoscale variability in oligotrophic environments: Biological production and community structure. *Journal of Geophysical Research*, *107*, 1–21.

Lindo-Atichati, D., Bringas, F., Goni, G., Muhling, B., Muller-Karger, F. E., & Habtes, S. (2012). Varying mesoscale structures influence larval fish distribution in the northern Gulf of Mexico. *Marine Ecology Progress Series*, *463*, 245–257.

Lohrenz, S. E., Fahnenstiel, G. L., Redalje, D. G., Lang, G. A., Dagg, M. J., Whitledge, T. E., & Dortch, Q. (1999). Nutrients, irradiance, and mixing as factors regulation primary production in coastal waters impacted by the Mississippi River plume. *Continental Shelf Research*, *19*, 1113–1141.

Meekan, M. G., Carleton, J. H., Steinberg, C. R., et al. (2006). Turbulent mixing and mesoscale distributions of late-stage fish larvae on the NW Shelf of Western Australia. *Fisheries Oceanography*, *15*, 44–59.

Misund, O., Luyeye, N., Coetzee, J., & Boyer, D. (1999). Trawl sampling of small pelagic fish off Angola: Effects of avoidance, towing speed, tow duration, and time of day. *ICES Journal of Marine Science*, *56*, 275–283.

Randall, L. L., Smith, B. L., Cowan, J. H., & Rooker, J. R. (2015). Habitat characteristics of bluntnose flyingfish *Prognichthys occidentalis* (Actinopterygii, Exocoetidae), across mesoscale features in the Gulf of Mexico. *Hydrobiologia*, *749*, 97–111.

Raya, V., & Sabates, A. (2015). Diversity and distribution of early life stages of carangid fishes in the northwestern Mediterranean: Responses to environmental drivers. *Fisheries Oceanography*, *24*, 118–134.

Roberts, J. J., Best, B. D., Dunn, D. C., Treml, E. A., & Halpin, P. N. (2010). Marine Geospatial Ecology Tools: An integrated framework for ecological geoprocessing with ArcGIS, Python, R, MATLAB, and C++. *Environmental Modelling and Software*, *25*, 1197–1207.

Rooker, J. R., Kitchens, L. L., Dance, M. A., Wells, R. J. D., Falterman, B., & Cornic, M. (2013). Spatial, temporal, and habitat-related variation in abundance of pelagic fishes in the Gulf of Mexico: Potential implications of the Deepwater Horizon Oil Spill. *PLoS One*, *8*, e76080.

Rooker, J. R., Simms, J. R., David Wells, R. J., Holt, S. A., Holt, G. J., Graves, J. E., & Furey, N. B. (2012). Distribution and habitat associations of billfish and swordfish larvae across mesoscale features in the Gulf of Mexico. *PLoS One*, *7*, e34180.

Seki, M. P., Polovina, J. J., Brainard, R. E., Bidigare, R. R., Leonard, C. L., & Foley, D. G. (2001). Biological enhancement at cyclonic eddies tracked with GOES thermal imagery in Hawaiian waters. *Geophysical Research Letters*, *28*, 1583–1586.

Shaw, R. F., & Drullinger, D. L. (1990). *Early-Life-History profiles, seasonal abundance, and distribution of four Species of Carangid larvae from the Northern Gulf of Mexico, 1982 and 1983*, NOAA NMFS Technical Report No. 89. 37p.

Shimose, T., & Wells, R. (2015). Feeding ecology of bluefin tunas. In T. Kitagawa, & S. Kumura (Eds.), *Biology and ecology of bluefin tunas* (pp. 78–97). Boca Raton, FL: CRC Press, Taylor and Francis Group.

Syahailatua, A., Taylor, M. D., & Suthers, I. M. (2011). Growth variability and stable isotope composition of two larval carangid fishes in the East Australian Current: The role of upwelling in the separation zone. *Deep-Sea Research Part II: Topical Studies in Oceanography*, *58*, 691–698.

Thorrold, S., & McKinnon, A. (1995). Response of larval fish assemblages to a riverine plume in coastal waters of the central great barrier reef lagoon. *Limnology and Oceanography*, *40*, 177–181.

Toner, M., Kirwan, A., Poje, A., Kantha, L., Muller-Karger, F., & Jones, C. (2003). Chlorophyll dispersal by eddy-eddy interactions in the Gulf of Mexico. *Journal of Geophysical Research*, *108*, 1–12.

Torres-Rojas, Y. E., Hernández-Herrera, A., Galván-Magaña, F., & Alatorre-Ramírez, V. G. (2010). Stomach content analysis of juvenile, scalloped hammerhead shark *Sphyrna lewini* captured off the coast of Mazatlan, Mexico. *Aquatic Ecology*, *44*, 301–308.

Troupin, C., Barth, A., Sirjacobs, D., et al. (2012). Generation of analysis and consistent error fields using the Data Interpolating Variational Analysis (DIVA). *Ocean Modelling*, *52–53*, 90–101.

Vukovich, F. M. (2007). Climatology of ocean features in the Gulf of Mexico using satellite remote sensing data. *Journal of Physical Oceanography*, *37*, 689–707.

Vukovich, F. M., & Crissman, B. W. (1986). Aspects of warm rings in the Gulf of Mexico. *Journal of Geophysical Research*, *91*, 2645–2660.

Walker, N. D., Wiseman, W. J., Rouse, L. J., & Babin, A. (2005). Effects of river discharge, wind stress, and slope eddies on circulation and the satellite-observed structure of the Mississippi River Plume. *Journal of Coastal Research*, *216*, 1228–1244.

Wiebe, P., Morton, A., Bradley, A., et al. (1985). New developments in the MOC, an apparatus for sampling zooplankton and micronekton. *Marine Biology*, *87*, 313–323.

Williams, A. K., Mcinnes, A. S., Rooker, J. R., & Quigg, A. (2015). Changes in microbial plankton assemblages induced by mesoscale oceanographic features in the northern Gulf of Mexico. *PLoS One*, *10*(9), e0138230. doi:10.1371/journal.pone.0138230.

Zimmerman, R. A., & Biggs, D. C. (1999). Patterns of distribution of sound-scattering zooplankton in warm- and cold-core eddies in the Gulf of Mexico, from a narrowband acoustic Doppler current profiler survey. *Journal of Geophysical Research*, *104*, 5251–5262.

## SUPPORTING INFORMATION

Additional Supporting Information may be found online in the supporting information tab for this article.

**How to cite this article:** Mohan JA, Sutton TT, Cook AB, Boswell KM, David Wells RJ. Influence of oceanographic conditions on abundance and distribution of post-larval and juvenile carangid fishes in the northern Gulf of Mexico. *Fish Oceanogr*. 2017;00:1–16. https://doi.org/10.1111/fog.12214